Fibers and Polymers 2005, Vol.6, No.2, 131-138

Constitutive Equations for Dilute Bubble Suspensions and Rheological Behavior in Simple Shear and Uniaxial Elongational Flow Fields

Dongjin Seo and Jae Ryoun Youn*

School of Materials Science and Engineering, Seoul National University, Seoul 151-742, Korea
(Received December 8, 2004; Revised February 7, 2005; Accepted February 14, 2005)

Abstract: A theoretical model is proposed in order to investigate rheological behavior of bubble suspension with large deformation. Theoretical constitutive equations for dilute bubble suspensions are derived by applying a deformation theory of ellipsoidal droplet [1] to a phenomenological suspension theory [2]. The rate of deformation tensor within the bubble and the time evolution of interface tensor are predicted by applying the proposed constitutive equations, which have two free fitting parameters. The transient and steady rheological properties of dilute bubble suspensions are studied for several capillary numbers (*Ca*) under simple shear flow and uniaxial elongational flow fields. The retraction force of the bubble caused by the interfacial tension increases as bubbles undergo deformation. The transient and steady relative viscosity decreases as *Ca* increases. The normal stress difference (NSD) under the simple shear has the largest value when *Ca* is around 1 and the ratio of the first NSD to the second NSD has the value of 3/4 for large *Ca* but 2 for small *Ca*. In the uniaxial elongational flow, the elongational viscosity is three times as large as the shear viscosity like the Newtonian fluid.

Keywords: Dilute bubble suspension, Bubble deformation, Interface tensor, Capillary number

Introduction

Foams, which are bubble suspensions, are widely used in industrial applications because there are many advantages of foamed materials, including low cost, light weight, enhanced thermal and electrical insulation, and high impact strength [3]. For example, polyurethane foams have been studied for various practical applications [4-10]. The bubble suspension that consists of gaseous bubbles in a Newtonian fluid exhibits complex rheological behaviors, such as elastic effects and shear- and time-dependent viscosity [11-14]. Deformation of bubbles in the suspension and rheological behaviors of the suspension can be characterized by two dimensionless parameters: the capillary number (*Ca*) and the volume fraction of bubbles (ϕ). The capillary number is defined as

$$Ca = \frac{\mu G R}{\Gamma} \tag{1}$$

where μ is the viscosity of the matrix, G is the shear rate, R is the radius of the undeformed spherical bubble, and Γ is the interfacial tension.

Frankel and Acrivos [15] derived a constitutive equation for a dilute emulsion by considering the creeping motion of a droplet in a uniform and time-dependent shearing flow. For the case of small deformation, they obtained the differential equation with the Jaumann derivative, which could be recasted in the form of a Jeffreys model [12]. According to their calculation results, the relative viscosity was represented as bwlow.

$$\eta_r = \frac{1+((6/5)Ca)^2+\phi(1-(12/5)Ca^2)}{1+((6/5)Ca)^2} \tag{2}$$

*Corresponding author: jaeryoun@snu.ac.kr

This equation reveals that the predictions by both Taylor and Mackenzie are the two limiting cases for small and large *Ca*, respectively. Schowalter *et al.* [16] presented for small *Ca* and small bubble deformation in a simple shear flow that the normalized first and the second normal stress differences (NSD) were $32\phi Ca/5$ and $-20\phi Ca/7$, respectively.

Some researchers performed theoretical investigations by considering a liquid drop as an ellipsoid. Maffettone and Minale [1] presented a phenomenological model for the droplet deformation in a fluid under a flow field with a uniform velocity gradient, but the model deviates from experimental results at large *Ca* and high viscosity ratios. Jackson and Tucker [17] combined the Eshelby model with the slender-body model to predict the transient shape evolution of an ellipsoidal Newtonian droplet with interfacial tension in a Newtonian fluid. Yu and Bousmina [18] also proposed an ellipsoidal model for droplet deformation in emulsions composed of two Newtonian fluids. These two models match the experimental results accurately under many types of flow fields.

Besides the theoretical approaches, there are some numerical and experimental studies to understand the rheological behavior of bubble suspensions. Due to the almost zero viscosity ratio of the gaseous bubble to the matrix, it is difficult to simulate the behavior of a bubble in a suspending fluid subject to a certain flow. Manga and Loewenberg [19] calculated the shear viscosity of a suspension of highly deformable bubbles dispersed within a Newtonian fluid. Boundary integral numerical techniques were employed to solve the bubble deformation at large *Ca*. Cristini *et al.* [20] carried out experiments and numerical simulations on the droplet deformation with the viscosity ratio of 0.1 at large *Ca*. They reported that the drop widening increased with increasing *Ca* and occurred when the viscosity ratio was less than unity. Cristini *et al.* [21]

studied the deformation and breakup of droplets under shear flow by using boundary integral simulation and experiments. They suggested accurate breakup criteria for a range of viscosity ratios. Renardy *et al.* [22] calculated droplet deformation under shear when a surfactant was present and the viscosity ratio was 0.05. They used the volume of fluid (VOF) algorithm to track interfaces with the structured Cartesian grid. Navier-Stokes equations were solved by a projection method and interface tension was modeled by a continuum method. They focused on the effects of surfactant concentration on the drop deformation and did not investigate the capillary number effects.

In this study, theoretical constitutive equations, which include the time evolution of bubble shape and orientation, are proposed to predict the rheological behavior of bubble suspensions for large bubble deformation at wide range of capillary numbers by applying a deformation theory of ellipsoidal droplet that was suggested by Maffettone and Minale [1] to a phenomenological suspension theory [2]. Studies on combining droplet deformation theory with suspension theory were carried out by some researchers [23]. In their studies, however, droplet relaxation by an interfacial tension and droplet deformation by an external flow were dealt with separately and viscosity difference between the matrix and the droplets was not considered. The relationship between the relative viscosity of the bubble suspension and the coefficients of Maffettone and Minale's model is derived in this study and used to overcome the mismatch between theoretical predictions and experimental measurements.

Theoretical Derivation of a Constitutive Equation

General Droplet Suspension Theory

Based on the general suspension theory, two immiscible and incompressible Newtonian fluids are considered. The suspension creates a complex flow, including the matrix (continuous phase) and the droplets (discontinuous phase) of various sizes and shapes. Following Landau and Lifshitz [24], the volume-averaged extra stress for the suspension of incompressible Newtonian fluids with zero interfacial tension can be represented as

$$\bar{\boldsymbol{\tau}}^{V} = 2\mu\bar{\mathbf{E}} + 2\phi(\mu^{*}-\mu)\bar{\mathbf{E}}^{*} \tag{3}$$

where $\bar{\mathbf{E}}$ is the volume-averaged rate-of-deformation tensor and the superscript * denotes the droplet phase. The volume used for averaging should be larger than the size of the microstructure, but small enough to cover the variation of structure. According to Doi and Ohta [2], the extra stress due to the interfacial tension can be considered as below.

$$\bar{\boldsymbol{\tau}}^{I} = -\Gamma\mathbf{q} \tag{4}$$

where $\mathbf{q}$ is called as the interface tensor defined as equation (5).

$$\mathbf{q} = \frac{1}{V}\int_{A}\left(\hat{\mathbf{n}}\hat{\mathbf{n}} - \frac{1}{3}\mathbf{I}\right)dA \tag{5}$$

Here V is the total system volume including a matrix and droplets, $\hat{\mathbf{n}}$ is the unit normal vector at the interface, and $\mathbf{I}$ is the unit tensor. The interface tensor can be related to the area tensor, which is proposed by Wetzel and Tucker [25].

$$\mathbf{q} = \mathbf{A} - \frac{1}{3}Q\mathbf{I} \tag{6}$$

Here $\mathbf{A}$ is the area tensor and Q is the invariant, $tr(\mathbf{A})$, which denotes the total interfacial area per unit volume.

The volume-averaged extra stress for dispersion of an incompressible Newtonian fluid can be expressed by considering the interfacial tension as follows.

$$\bar{\boldsymbol{\tau}} = 2\mu\bar{\mathbf{E}} + 2\phi(\mu^{*}-\mu)\bar{\mathbf{E}}^{*} - \Gamma\mathbf{q} \tag{7}$$

Equation (7) can be changed into a dimensionless form.

$$\tilde{\boldsymbol{\tau}} = 2\tilde{\mathbf{E}} + 2\phi(\lambda-1)\tilde{\mathbf{E}}^{*} - \frac{3\phi}{Cd}\tilde{\mathbf{q}} \tag{8}$$

where λ is the viscosity ratio ($= \mu^{*}/\mu$). Cd is the dynamic capillary number that denotes the ratio of the viscous dissipation energy to the interfacial energy, and is defined as

$$Cd = \frac{3\mu\dot{\gamma}\phi}{\Gamma Q} \tag{9}$$

where $\dot{\gamma}$ is the rate of deformation ($= \sqrt{2\bar{\mathbf{E}}:\bar{\mathbf{E}}}$), which becomes the shear rate G for a simple shear flow. If all droplets are assumed to be spherical and have the same radii, the radius of the spherical droplet (R) is equivalent with $3\phi/Q$ so that Cd equals to Ca. The dimensionless variables are defined as follows.

$$\tilde{\boldsymbol{\tau}} = \frac{\bar{\boldsymbol{\tau}}}{\mu\dot{\gamma}}, \quad \tilde{\mathbf{E}} = \frac{\bar{\mathbf{E}}}{\dot{\gamma}}, \quad \tilde{\mathbf{q}} = \frac{\mathbf{q}}{Q} \tag{10}$$

In addition, the relaxation time of the droplet is defined.

$$\tau = \frac{3\mu\phi}{\Gamma Q} = Cd/\dot{\gamma} \tag{11}$$

The relaxation time and the dynamic capillary number are inversely proportional to the interfacial area and will be changing continuously during droplet deformation. The expressions of the volume-averaged rate of deformation tensor within the droplets ($\tilde{\mathbf{E}}^{*}$), the evolution of the interface tensor ($\tilde{\mathbf{q}}$), and the interfacial area per unit volume (Q) under any flow field must be identified in order to evaluate equation (8).

The volume-averaged velocity gradient tensor within the droplets, in general, depends on the geometry of the droplets and the viscosity ratio λ. For an ellipsoidal droplet without interfacial tension, Wetzel and Tucker [25] provided a complete solution of velocity field by using the Eshelby tensor. Their

solution which is equal to the result of Frankel and Acrivos [15] is expressed as below for a dilute spherical droplet with small deformation.

$$\tilde{\mathbf{E}}^* = \frac{5}{2\lambda+3}\tilde{\mathbf{E}} \tag{12}$$

For concentrated dispersion of nearly spherical droplets without interfacial tension [26], $\tilde{\mathbf{E}}^*$ can be expressed by the following equation

$$\tilde{\mathbf{E}}^* = \frac{5}{2(1-\phi)\lambda+3+2\phi}\tilde{\mathbf{E}} \tag{13}$$

If the interfacial tension is not negligible, $\tilde{\mathbf{E}}^*$ is a function of not only the applied flow field but also the interfacial tension. Jackson and Tucker [17] and Yu and Bousmina [18] proposed equations of the velocity gradient tensor within an ellipsoidal droplet. The equations gave good predictions for wide range of the viscosity ratio but it is difficult for the equations to be applied to the bubble suspension. According to Maffettone and Minale [1], the volume-averaged velocity gradient tensor within an ellipsoidal droplet is proposed as

$$\tilde{\mathbf{L}}^* = \tilde{\mathbf{W}} + f_2\tilde{\mathbf{E}} + \frac{3f_1}{Ca}\left(\frac{\mathbf{G}}{tr(\mathbf{G})} - \frac{1}{3}\mathbf{I}\right) \tag{14}$$

where $\mathbf{G}$ is called as the shape tensor [17]. The shape tensor can be approximated by the area tensor (see Appendix A) and equation (14) can be changed to

$$\tilde{\mathbf{L}}^* \approx \tilde{\mathbf{W}} + f_2\tilde{\mathbf{E}} + \frac{3f_1}{Cd}\tilde{\mathbf{q}} \tag{15}$$

where $\tilde{\mathbf{L}}$ is the dimensionless velocity gradient tensor ($= \mathbf{L}/\dot{\gamma}$) and $\tilde{\mathbf{W}}$ is the dimensionless vorticity tensor ($= \mathbf{W}/\dot{\gamma}$). f_1 and f_2 are functions of the viscosity ratio.

$$f_1 = \frac{40(\lambda+1)}{(2\lambda+3)(19\lambda+16)} \tag{16}$$

$$f_2 = \frac{5}{(2\lambda+3)} \tag{17}$$

If equation (15) is substituted into equation (8), the dimensionless volume-averaged extra stress is obtained.

$$\tilde{\boldsymbol{\tau}} = 2[1+\phi(\lambda-1)f_2]\tilde{\mathbf{E}} - \frac{3\phi\kappa}{Cd}\tilde{\mathbf{q}} \tag{18}$$

$$\kappa = 1-2(\lambda-1)f_1 \tag{19}$$

Doi and Ohta [2] considered the equal viscosity mixtures and κ is unity in their equations. If λ is not equal to unity, κ is not equal to unity. κ represents the effect of viscosity difference on interfacial tension. Peters *et al.* [27] also suggested that the stress related to the viscosity difference was not purely viscous and proposed that $f_1 = 1/(2\lambda+3)$ for dilute spherical droplet suspensions. According to Graebling *et al.* [28], the relaxation time of a suspension of two Newtonian fluids is τ/f_1 for a nearly spherical droplet. The relaxation time corresponds to the time required for a deformed droplet to recover its spherical shape.

Time evolution of the area tensor for an incompressible homogeneous fluid without interfacial tension under a velocity field $\mathbf{L}$ can be expressed in a dimensionless form with a simple closure approximation (see Appendix B).

$$\frac{D\tilde{\mathbf{A}}}{D\tilde{t}} = -\tilde{\mathbf{L}}^T\cdot\tilde{\mathbf{A}} - \tilde{\mathbf{A}}\cdot\tilde{\mathbf{L}} + 2(\tilde{\mathbf{L}}:\tilde{\mathbf{A}})\tilde{\mathbf{A}} - \frac{2}{5}II_{\tilde{\mathbf{A}}}\tilde{\mathbf{E}} \tag{20}$$

where $\tilde{\mathbf{A}}$ is the normalized or dimensionless area tensor ($= \mathbf{A}/Q$), $\tilde{t}$ is the dimensionless time ($= t\dot{\gamma}$), $II_{\tilde{\mathbf{A}}}$ is the second invariant of area tensor, and the superscript T means transpose. If equation (6) is substituted into equation (20), the evolution equation of the interface tensor is obtained as follows.

$$\dot{\tilde{\mathbf{q}}} \equiv \frac{D\tilde{\mathbf{q}}}{D\tilde{t}} = -\tilde{\mathbf{L}}^T\cdot\tilde{\mathbf{q}} - \tilde{\mathbf{q}}\cdot\tilde{\mathbf{L}} - \frac{2}{15}(5+3II_{\tilde{\mathbf{A}}})\tilde{\mathbf{E}} + 2(\tilde{\mathbf{L}}:\tilde{\mathbf{q}})\left(\tilde{\mathbf{q}}+\frac{1}{3}\mathbf{I}\right) \tag{21}$$

For a suspension with interfacial tension and non-equal viscosity, it is proposed that $\tilde{\mathbf{L}}$ should be replaced with $\tilde{\mathbf{L}}^*$. It is not necessary to consider the flow effect and the interfacial tension effect separately because $\tilde{\mathbf{L}}^*$ contains these two effects. The following equation is obtained by combining equations (15) and (21).

$$\overset{\circ}{\tilde{\mathbf{q}}} = -\frac{2(5+3II_{\tilde{\mathbf{A}}})}{15}\left(f_2\tilde{\mathbf{E}} + \frac{3f_1}{Cd}\tilde{\mathbf{q}}\right) - f_2(\tilde{\mathbf{E}}^T\cdot\tilde{\mathbf{q}} + \tilde{\mathbf{q}}\cdot\tilde{\mathbf{E}}) - \frac{6f_1}{Cd}\tilde{\mathbf{q}}\cdot\tilde{\mathbf{q}} + 2\left(f_2\tilde{\mathbf{E}}:\tilde{\mathbf{q}} + \frac{3f_1}{Cd}\tilde{\mathbf{q}}:\tilde{\mathbf{q}}\right)\left(\tilde{\mathbf{q}}+\frac{1}{3}\mathbf{I}\right) \tag{22}$$

where $\overset{\circ}{\tilde{\mathbf{q}}}$ is the Jaumann derivative defined as below.

$$\overset{\circ}{\tilde{\mathbf{q}}} = \dot{\tilde{\mathbf{q}}} - \tilde{\mathbf{W}}\cdot\tilde{\mathbf{q}} + \tilde{\mathbf{q}}\cdot\tilde{\mathbf{W}} \tag{23}$$

If the same analogy is applied to the total interfacial area per unit volume, Q is evolved as follows.

$$\frac{DQ}{Dt} = -\mathbf{E}^*:\mathbf{q} = -f_2\mathbf{E}:\mathbf{q} - \frac{3f_1}{\tau Q}\mathbf{q}:\mathbf{q} \tag{24}$$

According to Lee and Park [29], there are three mechanisms of droplet relaxation: coalescence, shape relaxation, and break-up by interfacial tension. If equations (22) and (24) are compared with equations in the literature, the dimensionless constants of three modes for droplet relaxation are given: the total relaxation $\tau_\lambda = 2\phi f_1/3$, the size relaxation $\tau_\mu = 0$, and the breakup and shape relaxation $\tau_\nu = 2/3$. It is known that $\tau_\mu \sim 0$ and $\tau_\nu \sim 1$ when the shape relaxation dominates over the other relaxations in a dilute system. In this study, equations are proposed based on the model of Maffettone and Minale [1], who considered an ellipsoidal droplet in a viscous flow without breakup and coalescence, so that the

shape relaxation dominates. In the Lee and Park model, f_2 is unity despite the consideration of viscosity difference between the droplets and matrices. They simply combined the interfacial tension and the flow effects, but it must be corrected if there is the viscosity difference between the droplets and matrices. When equation (9) is substituted into equation (24), the evolution equation of the dynamic capillary number is obtained as follows.

$$\frac{D(Cd)}{D\tilde{t}} = f_2 Cd\tilde{\mathbf{E}}:\tilde{\mathbf{q}} + 3f_1\tilde{\mathbf{q}}:\tilde{\mathbf{q}} \tag{25}$$

Bubble Suspension

The liquid droplet suspension theories can be directly applied to bubble suspension where λ is zero. Equation (18) can be represented as

$$\tilde{\tau} = 2\eta_\alpha\tilde{\mathbf{E}} - \frac{3\phi}{Cd}\kappa\tilde{\mathbf{q}} \tag{26}$$

$$\eta_\alpha = 1 - \phi f_2 \tag{27}$$

where η_α is the relative viscosity of the bubble suspension when the interfacial tension is negligible. By substituting equation (17) into equation (27), the relative viscosity is evaluated as follows.

$$\eta_\alpha = 1 - \frac{5}{3}\phi \tag{28}$$

It is the same value as the result calculated by Mackenzie [30] for a dilute spherical droplet with small deformation.

If equations (22) and (26) are combined and $\tilde{\mathbf{q}}$ is eliminated in the combined equation by assuming that bubbles are nearly spherical ($Cd \to Ca$, $II_{\tilde{\mathbf{A}}} \to -1/3$, and $o \to \cdot$), the following equation is obtained.

$$\tilde{\tau} + \frac{5Ca}{8f_1}\overset{\nabla}{\tilde{\tau}} = 2\left(\eta_\alpha + \frac{f_2}{2f_1}\phi\kappa\right)\tilde{\mathbf{E}} + 2\eta_\alpha\frac{5Ca}{8f_1}\overset{\nabla}{\tilde{\mathbf{E}}} \tag{29}$$

The above equation has the same form as the linear viscoelastic Jeffreys model. According to the equation, the relaxation time of bubble suspensions is $5\tau/8f_1$ ($= 3\tau/4$), which is given as $6\tau/5$ in the similar equation derived by Llewellin *et al.* [12]. As mentioned before, Graebling *et al.* [28] suggested that the relaxation time of the suspension of two Newtonian fluid is τ/f_1 for nearly spherical droplet. This difference may result from the closure approximation and approximate conversion of the shape tensor into the area tensor. When $Ca << 1$, the above equation is simplified to

$$\tilde{\tau} = 2\left(\eta_\alpha + \frac{f_2}{2f_1}\phi\kappa\right)\tilde{\mathbf{E}} = \eta_\beta\tilde{\mathbf{E}} \tag{30}$$

where η_β is the relative viscosity of the bubble suspension at very small Ca. The relative viscosity is evaluated by applying equations (16) and (17) as follows.

$$\eta_\beta = 1 + \phi \tag{31}$$

It is the same result as the relationship derived by Taylor [31] for a dilute spherical droplet with small deformation.

The coefficients derived by Maffettone and Minale [1] are valid if a bubble suspension is dilute enough for coalescence to be prohibited. Even if the coefficients are obtained in the case of small deformation of bubbles, the three equations can be applied to the case of large deformation of bubbles because the model of Maffettone and Minale can predict droplet deformation if the droplet remains as an ellipsoid. But if the coefficient of Maffettone and Minale are invalid, the coefficients can be calculated by using the relative viscosity of bubble suspensions as follows.

$$f_1 = \frac{1 - \eta_\alpha}{2(\eta_\beta - 1)} \tag{32}$$

$$f_2 = \frac{1 - \eta_\alpha}{\phi} \tag{33}$$

$$\kappa = \frac{\eta_\beta - \eta_\alpha}{\eta_\beta - 1} \tag{34}$$

These equations are obtained from the equations (19), (27), and (30). Here η_α and η_β are the relative viscosity of the bubble suspension at large Ca and small Ca. Equations (22), (25), and (26) with these three coefficients are the final constitutive equations for the bubble suspension to be employed for theoretical prediction of the bubble suspension.

Results and Discussion

Simple Shear Flow

The constitutive equations proposed for bubble suspensions, equations (22), (25), and (26), were solved simultaneously under a simple shear flow for several capillary numbers. An Euler explicit method was used to obtain the exact solution of the differential equations. The interface tensor is set to be zero as an initial value because it is assumed that the bubble is spherical. Relative viscosities, η_α and η_β, are given as $(1 - 5\phi/3)$ and $(1 + \phi)$, respectively.

Figure 1 shows the transient variation of the relative viscosity for bubble suspensions with $\phi = 0.0625$ under a simple shear flow for several different capillary numbers. The solid lines are the results from the proposed model calculated by the Euler explicit method. The relative viscosity of every bubble suspension is less than unity initially, and then it increases as the bubble deforms and reaches its maximum value. Initially the relative viscosity has the value of $(1 - 5\phi/3)$ because the bubble deforms so slightly that the surface tension effects on the stress are negligible. As the bubble deforms further, the surface tension effects start to appear so that the viscosity of the suspension increases and reaches a certain plateau value, e.g., $(1 + \phi)$ if Ca is less than unity. When $Ca << 1$, the surface tension effects caused by the bubble anisotropy are so large and fast that the relative viscosity of the bubble

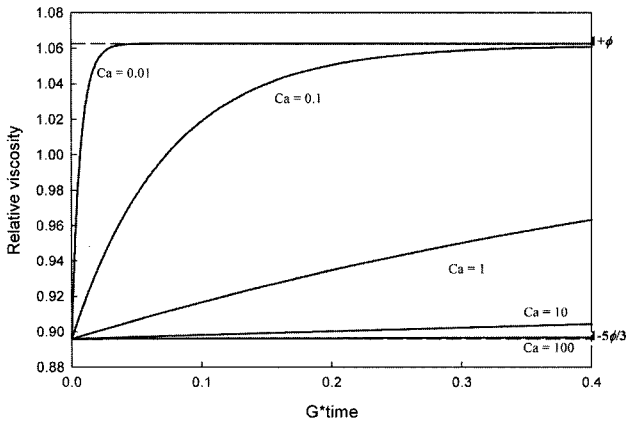

Figure 1. Transient variation of the relative viscosity for the bubble suspension with $\phi = 0.0625$ under a simple shear flow; upper and lower dashed lines are the analytic results for a dilute bubble suspension and solid lines are the results from the proposed model.

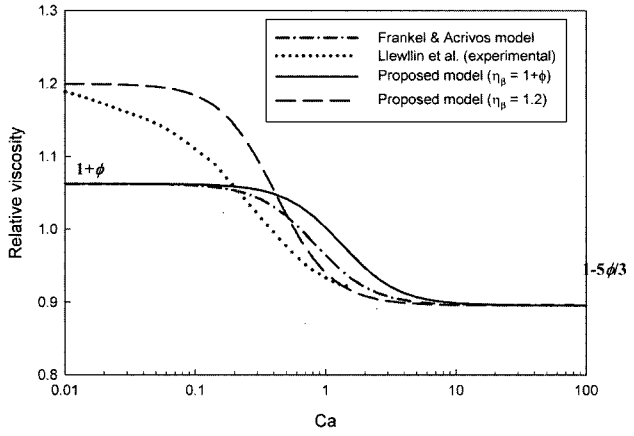

Figure 2. Relative viscosity with respect to the capillary number when bubbles are slightly deformed and $\phi = 0.0625$.

suspension is always greater than unity.

Figure 2 plots the relative viscosity with respect to Ca when bubbles are slightly deformed. The volume fraction of the bubble suspension is 0.0625. The relative viscosity predicted by the proposed theoretical model is compared with the results of the Frankel and Acrivos model [15] and the experimental results by Llewllin *et al.* [12]. When bubbles are nearly spherical and suspensions are dilute, the relative viscosity of bubble suspensions can be obtained from the constitutive equations as follows:

$$\tilde{\eta} = \frac{\eta_\beta + \eta_\alpha (5Ca/8f_1)^2}{1 + (5Ca/8f_1)^2} = \frac{1 + ((3/4)Ca)^2 + \phi(1 - (15/16))}{1 + ((3/4)Ca)^2} \tag{35}$$

Equation (35) is different from the relative viscosity calculated from the Frankel and Acrivos model given by equation (2). The relative viscosity of predicted by equation (35) is larger than that predicted by the Frankel and Acrovos model for capillary numbers ranging from 0.1 to 10. As shown in equation (29), the relaxation time of the proposed theoretical model differs from the other theoretical models that were derived mathematically by solving deformation of droplets in a certain flow. The difference in the relaxation time may come from the closure approximation and the approximate conversion of a shape tensor into an area tensor. Anyhow the relative viscosity of the bubble suspension decreases as the capillary number increases. The critical capillary number (Ca_{crit}), where bubble breakup occurs, is known to be greater than 1000 in a simple shear flow [32]. Since the change in the capillary number can be considered as that in the shear rate, the relative viscosity of the bubble suspension, in general, shows a shear thinning behavior.

The measured relative viscosity of the bubble suspension is usually larger than the value predicted by the theoretical models when $Ca << 1$ as shown in Figure 2, but the experimental data match the theoretical prediction $(1 - 5\phi/3)$ when $Ca >> 1$ [12-14,33]. One reason may be the hydrodynamic interaction between the bubbles even though they are not in direct contact each other. The flow field between bubbles becomes more complicated in the multiple bubble suspension than in the single bubble suspension. Another reason may come from rising of bubbles due to the buoyancy effect. Llewllin *et al.* [12] used a parallel plate viscometer to measure the relative viscosity. During the measurement it was observed that more bubbles were present below the upper plate than above the lower plate. When $Ca << 1$ the viscosity increase can be predicted by a simple treatment of the proposed model. If $\eta_\beta = 1.2$ $(= 1 + 3.2\phi)$ is substituted into the proposed theoretical model by using the relationships that are given in equations (32), (33), and (34), the model predicts the experimental results of Llewllin *et al.*[12] as shown in Figure 2. Some deviations at small capillary numbers may come from the polydispersity of the bubble sizes in their experiments.

The first and second normal stress differences (NSD) were obtained by using the phenomenological model proposed in this study. When bubbles are nearly spherical and suspensions are dilute, the normalized first and second NSD of bubble suspensions can be obtained from the constitutive equations as follows.

$$\tilde{\psi}_1 = \frac{2(5Ca/8f_1)(\eta_\beta - \eta_\alpha)}{1 + (5Ca/8f_1)^2} = \frac{4\phi Ca}{1 + ((3/4)Ca)^2} \tag{36}$$

$$\tilde{\psi}_2 = \frac{(5Ca/8f_1)(\eta_\beta - \eta_\alpha)}{1 + (5Ca/8f_1)^2} = -\frac{2\phi Ca}{1 + ((3/4)Ca)^2} \tag{37}$$

For small Ca and small deformation, Schowalter *et al.* [16] computed $\tilde{\psi}_1$ and $\tilde{\psi}_2$ as $32\phi Ca/5$ and $-20\phi Ca/7$, respectively. Figure 3 shows the transient variations of the first normal

stress difference for bubble suspensions with $\phi = 0.0625$ under the simple shear flow. The first NSD increases with the applied strain and reaches a certain maximum value. The first NSD has the largest value when the capillary number is around 1. As shown in the small figure inside Figure 3, the smaller the capillary number is the larger the first NSD at very small strain. The normal stress itself is very large but the interfacial tension makes the bubble shape be spherical so that the difference between the normal stresses is not large when $Ca << 1$. When $Ca >> 1$, the bubble deformation is very large and the interfacial tension is so small that the normal stress itself is not large.

Figure 4 shows the transient variations of the ratio of the first NSD to the second NSD for bubble suspensions with $\phi = 0.0625$ under a simple shear flow. The ratio is −3/4 at the small strain and increases as the applied strain does. For large Ca and small deformation, the ratio is calculated from

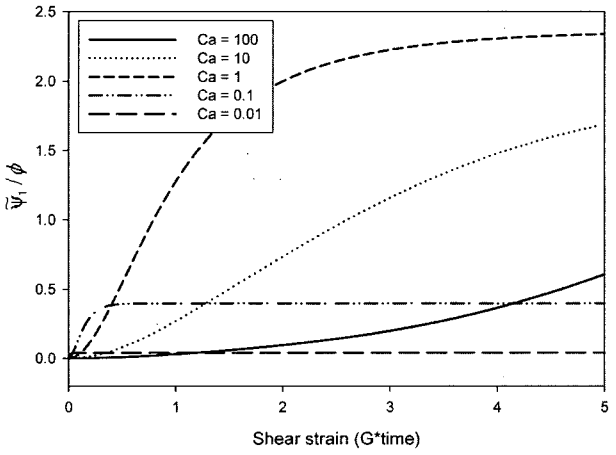

Figure 3. Transient variation of the first normal stress difference for the bubble suspension with $\phi = 0.0625$ under a simple shear flow.

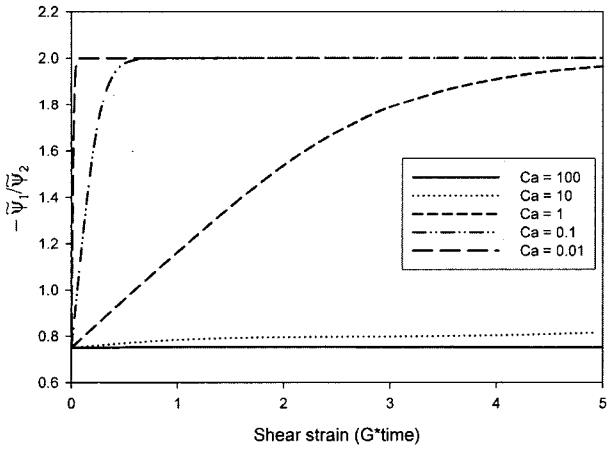

Figure 4. Transient variation of the ratio of the first normal stress difference to second normal stress difference for the bubble suspension with $\phi = 0.0625$ under a simple shear flow.

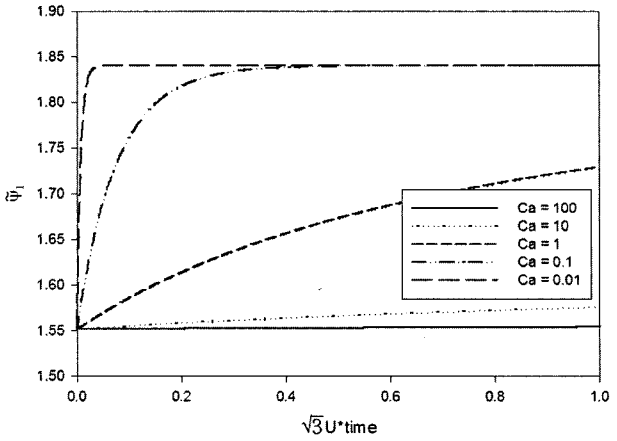

Figure 5. Transient variation of the normal stress difference for the bubble suspension with $\phi = 0.0625$ under a uniaxial elongational flow. U is the elongational rate.

our model as

$$\tilde{\psi}_1/\tilde{\psi}_2 = -2/(1+f_2) = -3/4 \tag{38}$$

It is peculiar that the second NSD is larger than the first NSD when $Ca >> 1$, which has not been reported yet and should be identified experimentally in the future. When Ca $<< 1$, the ratio reaches −2 at the small strain, which can be obtained from the equations (36) and (37).

Uniaxial Elongational Flow

Using the proposed phenomenological model, the normal stress difference is calculated for bubble suspensions with $\phi = 0.0625$ under the uniaxial elongational flow as shown in Figure 5. The velocity gradient tensor is given as

$$\mathbf{L} = \begin{pmatrix} U & 0 & 0 \\ 0 & -U/2 & 0 \\ 0 & 0 & -U/2 \end{pmatrix} \tag{39}$$

where U is the elongational rate. The normal stress difference can be calculated for the constitutive equations by using the assumption that bubbles are nearly spherical and suspensions are dilute.

$$\tilde{\tau}_{11} - \tilde{\tau}_{12} = \sqrt{3}\,\tilde{\eta} \tag{40}$$

Equation (40) is normalized by the shear rate that is $\sqrt{3}U$. The elongational viscosity of the bubble suspension is three times the shear viscosity like the Newtonian fluid.

Conclusions

A phenomenological constitutive equation that includes the time evolution of bubble size and orientation was proposed by applying the general suspension theory. The theory of

Maffettone and Minale was applied to the model in order to evaluate the rate of deformation tensor within the droplet and the time evolution of the interface tensor and the dynamic capillary number. The bubble deformation predicted by the proposed model was in good agreement with experimental results. In simple shear flow, the proposed theoretical model was employed to predict that the dynamic capillary number decreases as the bubbles deforms. The relative viscosity is less than unity in the case of very small bubble deformation and then increases as the bubbles deform. The relative viscosity decreases as the capillary number increases and its asymptotic values when $Ca >> 1$ and $Ca << 1$ agree well with the values predicted by other theoretical models. The relative viscosity predicted by the proposed model is larger than that predicted by the Frankel and Acrivos model for capillary numbers ranging from 0.1 to 10. The normal stress differences calculated by the model were different from those predicted by Schowalter *et al.* for small bubble deformation. The first NSD has the largest value when the capillary number is around 1 and the ratio of the first NSD to the second NSD has the value of 3/4 for large Ca but 2 for small Ca. In a uniaxial flow, the elongational viscosity is three times the shear viscosity like the Newtonian fluid.

Acknowledgements

This study was supported by the Korea Science and Engineering Foundation through the Applied Rheology Center (ARC), an officially KOSEF-created engineering research center at Korea University, Seoul, Korea.

References

1. P. L. Maffettone and M. Minale, *J. Non-Newt. Fluid Mech.*, **78**, 227 (1998).
2. M. Doi and T. Ohta, *Int. J. Chem. Phy.*, **95**(2), 1242 (1991).
3. D. Klempner and K. C. Frisch, "Handbook of Polymeric Foams and Foam Technology", Hanser Publishers, New York, 1991.
4. H. Park and J. R. Youn, *Journal of Engineering for Industry, ASME Transactions*, **114**(3), 323 (1992).
5. W. J. Cho, H. Park, and J. R. Youn, *Journal of Engineering Manufacture*, **208**, 121 (1994).
6. H. Park and J. R. Youn, *Polymer Engineering and Science*, **35**(23), 1899 (1995).
7. J. R. Youn and H. Park, *Polymer Engineering and Science*, **39**(3), 457 (1999).
8. C. Kim and J. R. Youn, *Polymer-Plastics Technology and Engineering*, **39**(1), 163 (2000).
9. M. S. Koo, K. Chung, and J. R. Youn, *Polymer Engineering and Science*, **41**(7), 1177 (2001).
10. W. H. Lee, S. W. Lee, T. J. Kang, K. Chung, and J. R. Youn, *Fibers and Polymers*, **3**(4), 159 (2002).
11. C. W. Macosko, "Rheology: Principles, Measurements, and Applications", p.425, Wiley, New York, 1994.
12. E. W. Llewellin, H. M. Mader, and S. D. R. Wilson, *Proceedings of the Royal Society of London Series A*, **458**, 987 (2002).
13. A. C. Rust and M. Manga, *J. Non-Newt. Fluid Mech.*, **104**, 53 (2002).
14. Y. M. Lim, D. Seo, and J. R. Youn, *Korea-Australia Rheology Jounal*, **16**(1), 47 (2004).
15. N. A. Frankel and A. Acrivos, *Journal of Fluid Mechanics*, **44**, 65 (1970).
16. W. R. Schowalter, C. E. Chaffey, and H. Brenner, *J. Colloid Interface Sci.*, **26**, 152 (1968).
17. N. E. Jackson and C. L. Tucker, *J. Rheol.*, **47**(3), 659 (2003).
18. W. Yu and M. Bousmina, *J. Rheol.*, **47**(4), 1011 (2003).
19. M. Manga and M. Loewenberg, *Journal of Volcanology and Geothermal Research*, **105**, 19 (2001).
20. V. Cristini, R. W. Hooper, C. W. Macosko, M. Simeone, and S. Guido, *Industrial & Engineering Chemistry Research*, **41**, 6305 (2002).
21. V. Cristini, S. Guido, A. Alfani, J. Blawzdziewicz, and M. Loewenberg, *J. Rheol.*, **47**, 1283 (2003).
22. Y. Y. Renardy, M. Renardy, and V. Cristini, *European Journal of Mechanics B/Fluids*, **21**, 49 (2002).
23. A. S. Almusallam, R. G. Larson, and M. J. Solomon, *J. Rheol.*, **44**, 1055 (2000).
24. L. D. Landau and E. M. Lifshitz, "Fluid Mechanics", p.76, Addison-Wesley Publishing Company, New York, 1959.
25. E. D. Wetzel and C. L. Tucker, *International Journal of Multiphase Flow*, **25**, 35 (1999).
26. J. F. Palierne, *Rheologica Acta*, **29**, 204 (1990).
27. G. W. M. Peters, S. Hansen, and H. E. H. Meijer, *J. Rheol.*, **45**(3), 659 (2001).
28. D. Graebling, R. Muller, and J. F. Palierne, *Macromolecules*, **26**, 320 (1993).
29. H. M. Lee and O. O. Park, *J. Rheol.*, **38**(5), 1405 (1994).
30. J. K. Mackenzie, *Proceedings of the Royal Society of London Series B*, **63**, 2 (1950).
31. G. I. Taylor, *Proceedings of the Royal Society of London Series A*, **138**, 41 (1932).
32. H. P. Grace, *Chemical Engineering Communications*, **14**, 225 (1982).
33. D. J. Stein and F. J. Spera, *Journal of Volcanology and Geothermal Research*, **49**, 157 (1992).
34. E. D. Wetzel and C. L. Tucker, *Journal of Fluid Mechanics*, **426**, 199 (2001).

Appendix A: Relationship Between Area Tensor and Shape Tensor

For an ellipsoidal droplet, the shape and orientation can be described by a shape tensor **G**. Every point on the surface of the droplet satisfies

$$\mathbf{x} \cdot \mathbf{G} \cdot \mathbf{x} = 1 \tag{A1}$$

where **x** is a position vector originating at the centroid of the droplet [34]. If the coordinate axes are set to be aligned with the principal axes of the droplet, a shape tensor (**G**) and an area tensor (**A**) are represented as

$$\mathbf{G} = \begin{bmatrix} 1/r_1^2 & 0 & 0 \\ 1 & 1/r_2^2 & 0 \\ 0 & 0 & 1/r_3^2 \end{bmatrix} \tag{A2}$$

where r_1, r_2, and r_3 are the principal axis lengths ($r_3 \geq r_2 \geq r_1$) and

$$\mathbf{A} = \begin{bmatrix} A_1 & 0 & 0 \\ 0 & A_2 & 0 \\ 0 & 0 & A_3 \end{bmatrix} \tag{A3}$$

where $A_1 \geq A_2 \geq A_3$. According to Wetzel and Tucker [25], the principal axis lengths and the diagonal components of an area tensor have the approximate relationship as follows:

$$\frac{r_1}{r_3} \cong \left(\frac{A_3}{A_1}\right)^{\alpha}, \quad \frac{r_1}{r_2} \cong \left(\frac{A_2}{A_1}\right)^{\alpha} \tag{A4}$$

where α is 0.5977. Therefore we can obtain

$$\tilde{\mathbf{G}} \cong \tilde{\mathbf{A}}^{2\alpha} \tag{A5}$$

where the tilde denotes the normalized variables. For mathematical convenience, this is further simplified as

$$\tilde{\mathbf{G}} \approx \tilde{\mathbf{A}} \tag{A6}$$

If a droplet is nearly spherical, equation (A6) is a good approximation.

Appendix B: Closure Approximation

In order to calculate the evolution equation of the second order area tensor, there is a need to evaluate the fourth order area tensor. There are many methods for closure approximation, such as quadratic closure, hybrid closure, and orthogonal closure. Especially Wetzel and Tucker [25] proposed RE closure that gives quite a good prediction for most of flow types but is impossible to manipulate mathematically. But in this study, a simple closure is derived. The fourth order area tensor is defined as

$$A_{ijkl} = \frac{1}{V}\int_A \hat{n}_i \hat{n}_j \hat{n}_k \hat{n}_k dA \tag{B1}$$

and its dimensionless form is represented as $\tilde{A}_{ijkl}$ ($= A_{ijkl}/Q$). The fourth order area tensor should obey the following conditions:

$$\tilde{A}_{ijkl} = \tilde{A}_{jikl} = \tilde{A}_{ijlk} = \ldots \tag{B2}$$

$$\tilde{A}_{iikl} = \tilde{A}_{kl} \tag{B3}$$

So a closure approximation is proposed as

$$\tilde{A}_{iikl} = \alpha(\delta_{ij}\delta_{kl}) + \beta(\delta_{ik}\delta_{jl} + \delta_{il}\delta_{jk}) + \gamma\tilde{A}_{ij}\tilde{A}_{kl} \tag{B4}$$

In order to satisfy equations (B2) and (B3), the coefficients α, β, γ should be

$$\alpha = \frac{1}{15}(\tilde{A}_{mn}\tilde{A}_{mn} - 1) = \frac{2}{15}II_{\tilde{\mathbf{A}}} \tag{B5}$$

$$\beta = -\frac{3}{2}\alpha \tag{B6}$$

$$\gamma = 1 \tag{B7}$$

Here $II_{\tilde{\mathbf{A}}}$ is the second invariant of the area tensor $\tilde{A}_{ij}$. Therefore the final closure is given

$$\tilde{A}_{iikl} = \frac{2}{15}II_{\tilde{\mathbf{A}}}\left[\delta_{ij}\delta_{kl} - \frac{3}{2}(\delta_{ik}\delta_{jl} + \delta_{il}\delta_{jk})\right] + \tilde{A}_{ij}\tilde{A}_{kl} \tag{B8}$$

The above equation is now called as the simple closure. If the equation is multiplied by the velocity gradient tensor, it becomes

$$\tilde{L}_{ij}\tilde{A}_{iikl} = -\frac{2}{5}II_{\tilde{\mathbf{A}}}\tilde{E}_{kl} + \tilde{L}_{ij}\tilde{A}_{ij}\tilde{A}_{kl} \tag{B9}$$

If a droplet shape is spherical, $II_{\tilde{\mathbf{A}}}$ is –1/3. It is the same equation as that proposed by Peters *et al.* [27]. But if the droplet is deformed significantly and its shape becomes a long circular cylinder, $II_{\tilde{\mathbf{A}}}$ is –1/4, so it gives different value from that given by Peters et al. If the shape of the droplet is lamellar as reported by Cristini *et al.* [20] in the case of droplet deformation under a strong shear flow, $II_{\tilde{\mathbf{A}}}$ is zero so that the simple closure becomes the quadratic closure.